

Institute of Pharmacology & Toxicology<sup>1</sup>, College of Pharmaceutical Sciences, Zhejiang University, Hangzhou  
Topharman Shanghai Co. Ltd.<sup>2</sup>, Shanghai, People's Republic of China

## Bortezomib induces apoptosis in human neuroblastoma CHP126 cells

PEIHUA LUO<sup>1</sup>, MEIHUA LIN<sup>1</sup>, MEILI LIN<sup>1</sup>, DIFENG ZHU<sup>1</sup>, ZHEN WANG<sup>2</sup>, JINGSHAN SHEN<sup>2</sup>, BO YANG<sup>1,\*</sup>, QIAOJUN HE<sup>1,\*</sup>

Received July 6, 2009, accepted July 7, 2009

Prof. Qiaojun He, Institute of Pharmacology & Toxicology, College of Pharmaceutical Sciences, Zhejiang University, Hangzhou 310058, People's Republic of China  
qiaojunhe@zju.edu.cn

\*Both authors contributed equally to this work.

Pharmazie 65: 213–218 (2010)

doi: 10.1691/ph.2010.9693

Neuroblastoma (NB), the most frequent solid tumor of early childhood, is diagnosed as a disseminated disease in >60% of cases, and several lines of evidence support the resistance to apoptosis as a prerequisite for NB progression, and new treatment modalities or potent drugs are further needed. Bortezomib owns a substantial cytotoxicity through regulating degradation of protein associated with cell cycle control and tumor growth. The involvement of bortezomib in neuroblastoma is largely unknown. The aim of this study was to investigate the effects and mechanisms of bortezomib on human neuroblastoma CHP126 cells. Our results indicated that bortezomib inhibits proliferation of neuroblastoma cells in a time- and dose- dependent manner, and the concentration that caused 50% inhibition of CHP126 cells growth was 11.25 nM. Furthermore, bortezomib-induced proliferation inhibition results from massive cell death characterized by apoptosis. Besides, the NF $\kappa$ B pathway was not involved in bortezomib treatment in neuroblastoma CHP126 cells, bortezomib-driven apoptotic events were associated with promoting p21 and Bax expression and down-regulating Bcl-2 expression. Ultimately, caspase-3 was activated and the cleavage of PARP was induced. Above all, our data revealed that bortezomib triggered apoptosis by enhancing the caspase 3 activation and/or modulating the Bax/Bcl-2 balance, and also provided preliminary data for further researches of bortezomib on pediatric neuroblastoma.

### 1. Introduction

The proteasome is a multicatalytic proteinase complex and plays a critical role in regulating the degradation of proteins crucial to cell cycle regulation and programmed cell death, or apoptosis. Dysregulating such proteins lead to tumor growth and cause cells to undergo apoptosis (Voorhees et al. 2003). Proteasome inhibition holds promise as a novel approach to the treatment of cancer as transformed cells display greater susceptibility to proteasome inhibition than nonmalignant cells. Inhibitors of the proteasome impact on cells in part through down-regulation of nuclear factor  $\kappa$ B and modulation of cell cycle proteins and other pro- and anti-apoptotic pathways (Zhang et al. 2009).

Bortezomib, also known as Velcade or PS341, is a dipeptide boronic acid analogue which is the first such inhibitor to undergo clinical testing. As demonstrated before, it has impressive antitumor activity in multiple myeloma therapy. Generally, bortezomib plays its role through targeting the 26S proteasome and induces cell death through down-regulation of nuclear factor  $\kappa$ B, modulation of cell cycle proteins and other pro- and anti-apoptotic proteins (Zhang et al. 2009; Adams et al. 1999). The mechanisms to clarify the antitumor effects of bortezomib, *in vitro* and *in vivo*, allow additional refinement of cancer therapy (Hengartner et al. 2000).

Apoptosis, or programmed cell death, is a highly regulated process that involves activation of a series of molecular events leading to cell death (Fulda and Debatin 2003). Several pathways have been described regulating apoptosis during development, tumorigenesis, and chemical treatments. The expression of several genes has been demonstrated to be critical for the regulation of apoptosis such as caspase cascades and Bcl-2 family proteins. Activation of the caspase cascade is involved in chemical- and agent-induced apoptosis. Activated caspase 9 cleaves and activates the executioner caspase 3 from the inactive pro-caspase 3 (Armstrong et al. 2008).

Neuroblastoma (NB) is the most frequent solid extracranial malignancy in children which is originated from improper differentiation of the neural crest cells. Whereas localized tumors in young infants often spontaneously regress or mature in response to treatments, the outcome of high-risk NB, incurable in 60% of cases, remains poor and poses a major therapeutic challenge in pediatric oncology, and new treatment modalities or potent drugs are further needed (Maris and Matthay 1999). Previous data revealed that multiple myeloma cell lines exhibited varying response patterns with bortezomib alone and in combination with other drugs. However, the effect and mechanisms of bortezomib on neuroblastoma cells are largely unknown. Our study was aimed to investigate the effects and mechanisms of bortezomib in human neuroblastoma CHP126 cells, and sup-

port the molecular basis for therapy of bortezomib in neuroblastoma.

## 2. Investigations, results and discussion

### 2.1. Bortezomib caused growth arrest in human neuroblastoma CHP126 cells in vitro

The cytotoxicity of bortezomib in CHP126 cells was determined by MTT assay, and treatment with bortezomib for 72 h induced dramatic cell growth inhibition with an  $IC_{50}$  value of 11.25 nM. For further examining the anti-proliferation activity of bortezomib on human neuroblastoma CHP126 cell, cell growth curve was performed with bortezomib (5, 10, 20 nM) for 24, 48, 72 h. The results shows that bortezomib caused dramatic cell growth inhibition in CHP126 cell in a time- and dose- dependent manner (Fig. 1).

### 2.2. Bortezomib induced apoptosis in CHP126 cells

To determine whether bortezomib induced growth arrest was associated with cell cycle arrest, PI staining and flow cytometry analysis were performed. Cells were treated with bortezomib (5, 10, 20 nM) for 72 h, and the results revealed that bortezomib failed to induce cell cycle arrest in CPH126 cells (Fig. 2A). Meanwhile DAPI staining and flow cytometry upon Annexin V-fluorescein isothiocyanate/PI staining were used to confirm whether bortezomib induced growth arrest was associated with apoptosis. Normal morphology were observed in control group, while, fragmented chromatin and apoptotic bodies were

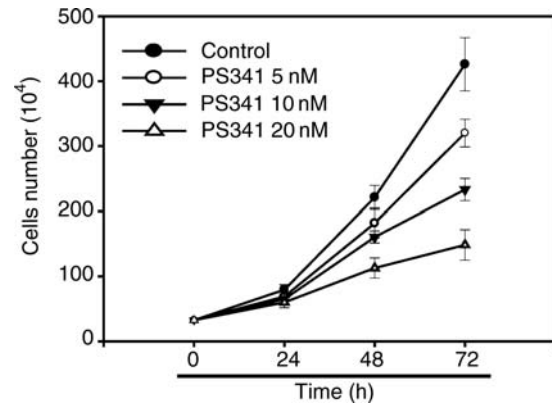


Fig. 1: Bortezomib induced growth arrest in human neuroblastoma CHP126 cells. Cells were exposed to Bortezomib (5–20 nM) for the indicated time points. Cell growth curve was performed by counting cells each day. Data are mean  $\pm$  SD (n = 3)

observed in cells treated with bortezomib by DAPI staining (Fig. 2B). Furthermore, it was shown that bortezomib induced apoptosis in a dose dependent manner in CHP126 cells, with the percentages of apoptosis accounted for 14.6%, 39.6%, and 58.2%, respectively, while the percentage of control group was 11.6% (Fig. 2C upper panel) by flow cytometry analysis. In addition, cells were exposed to 20 nM bortezomib for 6, 12, 24, 48 and 72 h, the results illustrated that bortezomib started to induce apoptosis of cells when treated with bortezomib (20 nM) for 48 h, and these results were consistent with the DAPI staining. All the results above suggested that apoptosis were responsive for bortezomib induced growth arrest in CHP126 cells.

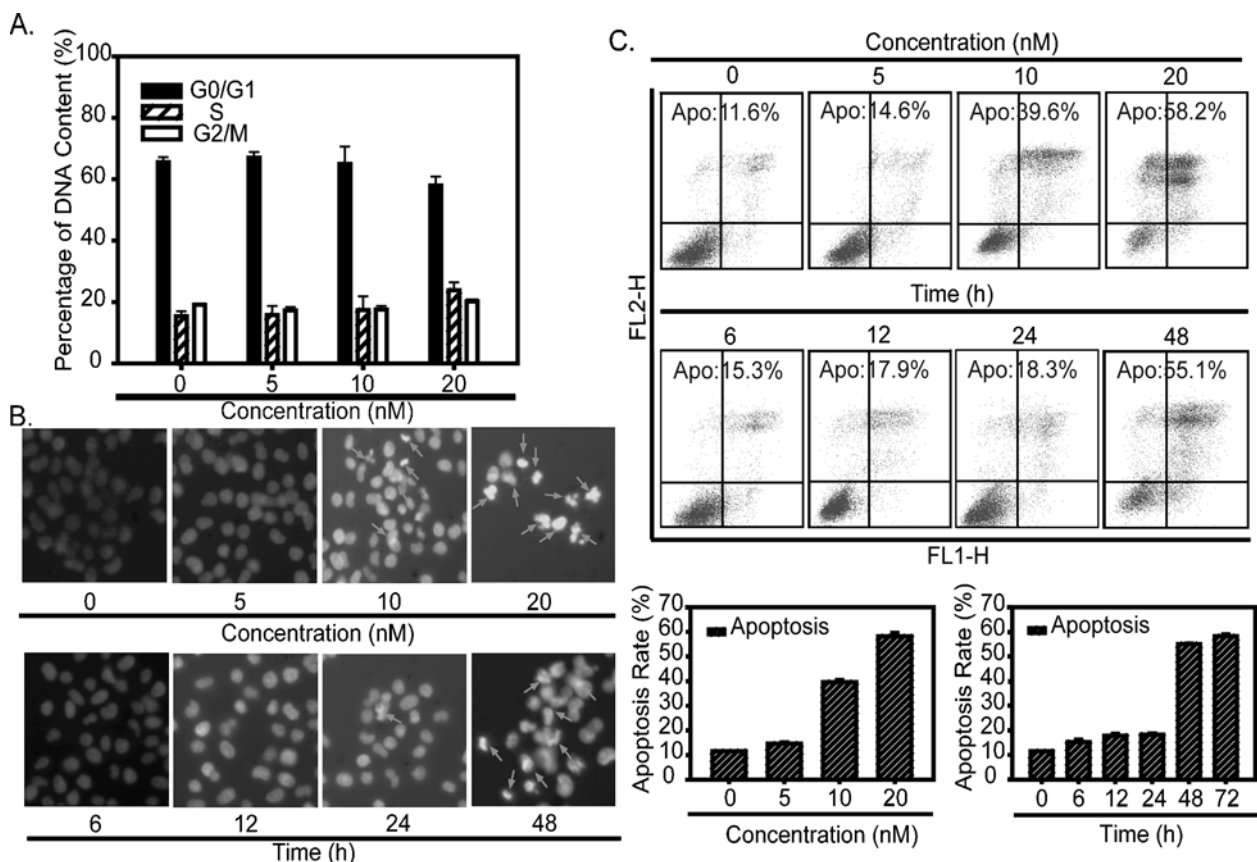


Fig. 2: Bortezomib induced apoptosis in human neuroblastoma CHP126 cells. (A) PI staining for flow cytometry. Cells were treated with bortezomib (5, 10, 20 nM) for 72 h, cells were analyzed using FACS after fixed by 70% ethanol and stained with PI. (B) DAPI staining. Cells were treated with Bortezomib (5, 10, 20 nM) for 72 h (upper panel), or treated with Bortezomib (20 nM) for 6, 12, 24, 48 h (lower panel), and stained with DAPI. Cells were observed by fluorescence microscopy at the same magnification (original magnification, 100 $\times$ ). Apoptotic nuclei were identified by condensed chromatin as well as nuclear fragmentation (arrows). Microphotographs shown are representative of three different experiments. (C) Annexin V-fluorescein isothiocyanate/PI staining for flow cytometry. After treatment, cells were harvested and stained with Annexin V-fluorescein isothiocyanate/PI. Flow cytometry was performed to quantify the percentages of apoptotic cells. Data are mean  $\pm$  SD

### 2.3. Bortezomib failed to activate NF $\kappa$ B pathway but with a dramatic promotion of p21 expression

As demonstrated before, bortezomib induces cell death through down-regulation of nuclear factor  $\kappa$ B, modulation of cell cycle proteins and other pro- and anti- apoptotic proteins (Hengartner 2000). Firstly, immunoblotting was performed to detect the expression of NF $\kappa$ B (p65) in nuclear and the I $\kappa$ B and p-I $\kappa$ B in plasma when treated with bortezomib in CHP126 cells. The result revealed that bortezomib failed to decrease the NF $\kappa$ B (p65) protein expression in nuclear or increase the expression of I $\kappa$ B and p-I $\kappa$ B proteins in plasma (Fig. 3A). From above, we inferred that a conventional NF $\kappa$ B pathway was not involved in bortezomib induced apoptosis in CHP126 cells. Secondly, as previous illustrated that cell cycle proteins play a vital role in bortezomib treatment. However, to be a potent inhibitor of cyclin-dependent kinases, p21 plays key role in growth arrest and cell death (Yu et al. 2008; Gartel and Tyner 2002). Thus, cells were exposed to bortezomib (5, 10, 20 nM) for 72 h or 20 nM bortezomib for 6, 12, 24, 48 and 72 h, immunoblotting and real-time quantitative PCR assay were used to detect the expression of p21 both in protein and mRNA level. The results demonstrated that bortezomib treatment caused p21 accumulation in a dose and time dependent manner in CHP126 cells (Fig. 3B and C). And the expression of p21 increased approximately 3-fold in protein level when treated with bortezomib (20 nM, 48 h), together with up to 60 folds in mRNA level when treated with bortezomib (20 nM, 72 h) (Fig. 3B and C).

### 2.4. Bortezomib induce Bax upregulation leads to caspase-3 activation and PARP cleavage

A previous study exhibited that p21 upregulation promotes the expression of Bax and accelerates apoptosis (Sheikh 1996). Bcl-2 family consists of pro- and anti-apoptotic proteins that modulate the execution phase of the cell death pathway. Bcl-2 acted as repressor of apoptosis while pro-apoptotic members acted as promoters (Kang 1999). Therefore, the ratio of Bax:Bcl-2 is a decisive factor for apoptosis threshold. After treatment, immunoblotting was performed, and the results indicated that Bax was markedly increased together with a decrease of Bcl-2 in protein level, thus, leading to an increase of the ratio of Bax over Bcl-2 (Fig. 4A). What's more, caspase cascade plays a crucial role in mitochondrial dysfunction associated apoptosis. So, we detected the caspase cascade pathway to further determine bortezomib induced cell death. And the results revealed that obvious proteolytic cleavage of caspase-3 was detected and subsequently, with PARP cleavage with Immunoblotting when treated with 20 nM bortezomib for 72 h in CHP126 cells (Fig. 4B). The results indicated that bortezomib induced CHP126 apoptosis through regulating Bcl-2 family on the upstream, and activated caspase-3 pathway after mitochondrial dysfunction, on the downstream.

## 3. Discussion

Human neuroblastoma is the major cause of death in infancy with neoplasia and is the most common solid extracranial malignancy in children (Maris and Mattay 1999). One of the hallmarks of malignant cell transformation and tumor development is a dysregulation of cellular proliferation and apoptosis (Fulda and Debatin 2003). In proliferation assays, dramatic cell growth arrest was observed in a time- and dose-dependent manner with bortezomib treatment.

As many previous data indicated that apoptosis was responsive to bortezomib-mediated anti-tumor activities, which is a distinct, intrinsic cell death program that occurs in various

physiological and pathological situations characterized by typical morphological and biochemical hallmarks including cell shrinkage, nuclear DNA fragmentation and membrane blebbing (Hengartner 2000). To detect whether bortezomib could induce apoptosis in human neuroblastoma CHP126 cells or not, flow cytometry upon PI staining and Annexin V-fluorescein isothiocyanate/PI staining assay was performed. And the results demonstrated that bortezomib failed to induce cell cycle arrest but with obvious apoptosis in a time- and dose-dependent manner. With DAPI staining, internucleosomal DNA fragmentation confirmed that apoptosis was responsive for bortezomib induced growth inhibition in CHP126 cells.

As illustrated before, bortezomib exhibits a treatment strategy targeting the 26S proteasome, a component of the ubiquitin-proteasome complex responsible for the degradation of unwanted cellular proteins and induces cellular apoptosis characterized by accumulating inhibitor of nuclear factor  $\kappa$ B (I $\kappa$ B) and preventing NF $\kappa$ B entering into the nucleus, so as to inhibit the expression of genes associated to the promotion of tumorigenesis (Zhang et al. 2009). However, in our experiment, bortezomib failed to accumulate I $\kappa$ B and p-I $\kappa$ B in plasma or block translocation of NF $\kappa$ B into the nucleus. To determine whether bortezomib induced apoptosis in CHP126 cells was mediated by NF $\kappa$ B pathway, we detected the expression level of I $\kappa$ B and p-I $\kappa$ B in plasma and NF $\kappa$ B (p65) in nuclear. The result revealed that NF $\kappa$ B pathway was not involved in bortezomib induced apoptosis in CHP126 cells, as there was no accumulation of I $\kappa$ B or p-I $\kappa$ B in plasma as well as decrease of NF $\kappa$ B translocation into the nucleus.

Nevertheless, bortezomib could modulate cell cycle proteins expression and induce apoptosis through regulating pro- and anti-apoptotic proteins. p21, a potent inhibitor of cyclin-dependent kinases, plays a key role in growth arrest in a p53-dependent or independent manner and induces apoptosis through blocking DNA replication (Yu et al. 2008; Gartel and Tyner 2002). A previous paper also reported that okadaic acid induced p21 upregulation failed to induce cell cycle arrest and it suggested that p21 possesses proapoptotic functions through increasing drug sensitivity and triggers cell apoptosis through regulating apoptotic associated proteins. In our study, the results demonstrated that p21 was dramatically increased both in protein and mRNA level in CHP126 cells when treated with bortezomib, which means that p21 might play a crucial role in bortezomib induced apoptosis. However, as reported before, overexpression of p21 up-regulates C<sub>6</sub>-ceramide-induced apoptosis in the human hepatoma Hep3B cells, and okadaic acid induced p21 upregulation failed to induce cell cycle arrest and suggested that p21 possesses proapoptotic functions through increasing drug sensitivity and triggers cell apoptosis through regulating apoptotic associated proteins and further study exhibited that p21 upregulation promotes the expression of Bax and modulates the molecular ratio of Bax:Bcl-2, thereby accelerating apoptosis (Gartel and Tyner 2002; Sheikh et al. 1996; Kang et al. 1999).

It is well known that the Bcl-2 family consists of pro-(Bax, Bad, Bak, Bid) and anti-apoptotic (Bcl-2, Bcl-xL, Mcl-1) proteins that modulate the execution phase of the cell death pathway. Anti-apoptotic members such as Bcl-2 act as repressor of apoptosis by blocking the release of cytochrome c, while proapoptotic members acts as promoters (Maheshwari et al. 2009). To elucidate the further role of p21 in bortezomib induced apoptosis in neuroblastoma CHP126 cells, immunoblotting was performed to detect the expression of Bcl-2 and Bax. The results confirmed that Bax was dramatically promoted with bortezomib treatment, leading to increase the ratio of Bax over Bcl-2. Besides, it is reported that overexpression of the pro-apoptotic molecule Bax is sufficient to induce cell death through caspase cascade activation together

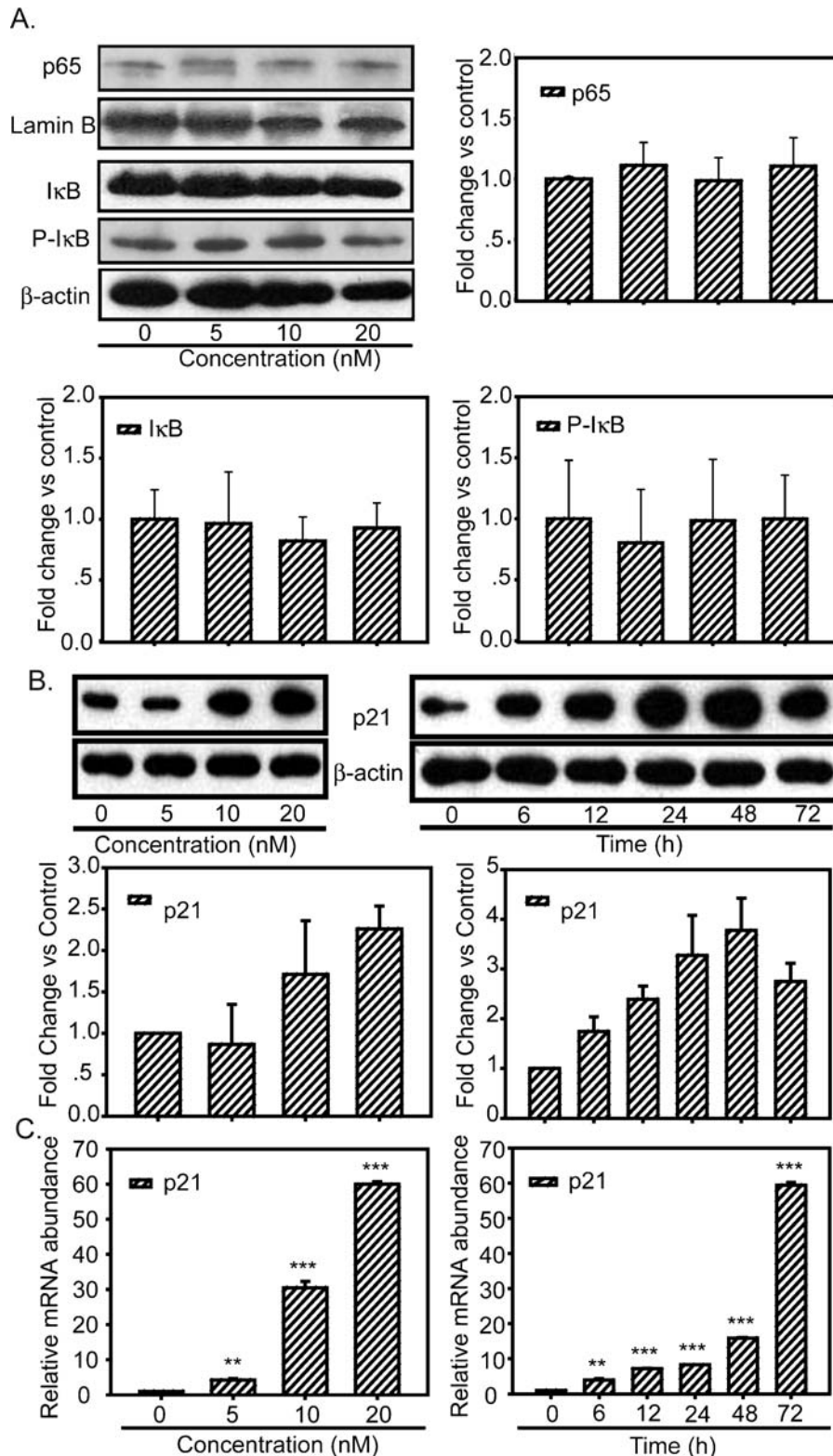


Fig. 3: Bortezomib induced apoptosis failed to activate NFκB pathway but with a dramatic promotion of p21 in protein and mRNA level. Nuclear lysates were extracted and immunoblotted with antibodies p65, and internal control, Lamin B (A). Whole-cell lysates were prepared and immunoblotted with p-Iκb, Iκb and internal control β-actin antibodies. (B) Real-time quantitative PCR. Total RNA of the cells were extracted following the kit and real-time PCR was performed to detect the expression of p21 gene (the folds of p21 mRNA were normalized to GAPDH mRNA). (C) After treatment, cells were harvested and whole-cell lysates were prepared and immunoblotted with p21 and β-actin antibodies. Data are mean ± SD (n=3), \*, p<0.01; \*\*\*, p<0.005 versus control

with mitochondrial dysfunction (Gross et al. 1998; Kim et al. 2006). To further elucidate whether Bax overexpression could induce apoptosis in neuroblastoma CHP126 cells, immunoblotting was performed to determine whether caspase cascade and the PARP was involved when treated with bortezomib. PARP is suggested to contribute to cell death by depleting the cell of

NAD and ATP with cleaving into 89- and 24-kDa fragments during drug-induced apoptosis in a variety of cells. Caspase-3 is primarily responsible for the cleavage of PARP during cell death and plays a key role in the execution of the apoptotic program (Boulares et al. 1999). The results confirmed that bortezomib treatment (20 nM, 72 h) efficiently induced a cleavage

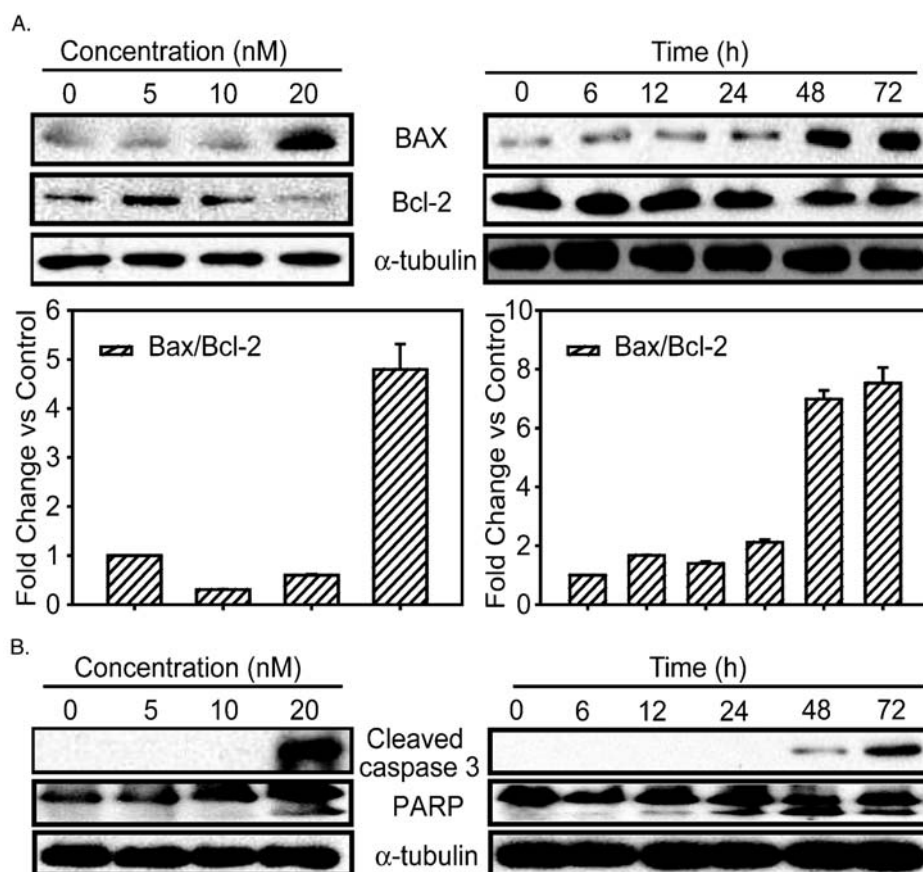


Fig. 4: Bortezomib Induce Bax upregulation leads to caspase-3 activation and PARP cleavage. Bortezomib induced Bax upregulation and increased the ratio of Bax: Bcl-2 leading to caspase activation and PARP cleavage in CHP126 cells. Cells were harvested after treatment by Bortezomib as indicated and whole-cell lysates were prepared and immunoblotted with Bax, Bcl-2 and internal control,  $\beta$ -tubulin antibodies (A) and cleaved caspase-3 and PARP as well as  $\beta$ -tubulin antibodies (B)

of 85 kDa of inactive intermediate band of PARP together with a cleavage of caspase-3. These results confirmed that bortezomib induced apoptosis was mediated with Bax induced apoptosis characterized with PARP cleavage and caspase-3 activation. Thus, the study revealed that bortezomib-induced apoptosis was mediated by enhancing the expression of p21, and subsequently promoting Bax expression, thereby increasing the molecular ratio of Bax:Bcl-2 in human neuroblastoma cells, so as to regulated mitochondria on the upstream, and activated caspase-3 pathway after mitochondrial dysfunction, on the downstream. All the data demonstrated that bortezomib was a potent compound against neuroblastoma and illustrate its mechanism for the first time.

## 4. Experimental

### 4.1. Reagents

Bortezomib was purchased from Topharman (Topharman, Shanghai, China), and dissolved in DMSO (1.0 mM stock solution) and stored at  $-20^{\circ}\text{C}$ . The primary antibodies to p-I $\kappa$ B, Bcl-2, Bax, p21, Lamin B,  $\beta$ -actin,  $\alpha$ -tubulin and HRP-labeled secondary anti-goat, anti-mouse, and anti-rabbit antibodies were all purchased from Santa Cruz Biotechnology (Santa Cruz, USA). The primary antibodies to NF $\kappa$ B(p65) and I $\kappa$ B were purchased from Cell Signaling Technology (Cell Signaling, MA). ECL was purchased from Amersham Biosciences (Piscataway, NJ). Fluorescein isothiocyanate-conjugated Annexin V and propidium iodide (PI) were both purchased from BD (Biosciences Pharmingen, San Diego, CA).

### 4.2. Cell culture

Human CHP126 cells were gifts from University of South California, and cultured in RPMI1640 (Invitrogen) supplemented with 10% fetal bovine serum (Invitrogen) containing 100 U/ml penicillin and 100  $\mu\text{g}/\text{ml}$  streptomycin (Sigma-Aldrich), and incubated at  $37^{\circ}\text{C}$  in a humidified 5%  $\text{CO}_2$  atmosphere (Wang et al. 2009).

### 4.3. Cytotoxicity assay

The cytotoxic activity of bortezomib on human neuroblastoma CHP126 cell line was measured using the thiazolyl blue (3-[4,5-dimethylthiazol-2-yl]-2,5-diphenyl tetrazolium bromide; MTT) assay. After treatment (3.125–100 nM PS341 for 72 h) in 96-well plates, MTT solution (5.0 mg/ml in RPMI 1640 medium; Sigma-Aldrich) was added (20.0  $\mu\text{l}/\text{well}$ ), and plates were incubated at  $37^{\circ}\text{C}$  for 4 h. The purple formazan crystals were dissolved in 100.0  $\mu\text{l}$  DMSO, and plates were read on an automated microplate spectrophotometer (Bio-Tek Instruments, USA) at 570 nm. The experiments were repeated three times with three replicates each. The concentration of drug inhibit for 50% of cells ( $\text{IC}_{50}$ ) was calculated using the software of dose-effect analysis with microcomputers (Fang et al. 2007).

### 4.4. Cell growth curve

For proliferation studies, equal numbers of cells were plated onto 6-well plates in triplicate. Twenty-four hours after plating, cells were exposed with 20 nM bortezomib for various times (0–72 h), or for 72 h treatment with bortezomib (0–20 nM). Cell growth curve was performed by counting cells each day. The experiments were repeated three times with three replicates each.

### 4.5. Flow cytometric analysis of DNA content and apoptosis

To detect the DNA content, cells were harvested after treatment, washed with PBS, and fixed with 70% ethanol. And resuspended in 100  $\mu\text{l}$  of PBS containing 50.0 mg/ml RNase (Amersco, USA), then incubated at  $37^{\circ}\text{C}$  for 1 h. After incubation, the cells were stained with 200.0 mg/ml PI at  $4^{\circ}\text{C}$  for 30 min. Flow cytometry was performed on FACScan (BD Biosciences, USA), with collection and analysis of data performed using CellQuest software (BD Biosciences) (Fang et al. 2007).

Annexin V-fluorescein isothiocyanate/PI is sensitive in detecting very early stages of the apoptotic process, and it allows precise quantification of apoptotic cells through flow cytometric analysis. After treatment, cells were harvested, washed, and resuspended with PBS. Fluorescein isothiocyanate-conjugated Annexin V and PI were added at manufacturer's recommended concentrations to 100.0  $\mu\text{l}$  aliquots containing  $1 \times 10^5$  cells. Cells were incubated for 15 min at  $18^{\circ}\text{C}$  in the dark. Cell suspensions were

diluted with 400.0 µl of binding buffer, and then they were analyzed by flow cytometry within 1 h. Flow cytometry was performed on FACScan (BD Biosciences, USA), with collection and analysis of data performed using CellQuest software (BD Biosciences) (Ying et al. 2008).

#### 4.6. DAPI staining assay

Cells were plated in 96-well culture plates. After treatment, cells were fixed with 4% paraformaldehyde for 30 min. Cells were washed with PBS, and incubated with 2 µl DAPI (5 µg/ml) for 5 min. Cells were examined using fluorescence microscopy. Cells with condensed chromatin or fragmented nuclei were considered apoptotic (Hotz et al. 1994).

#### 4.7. Immunoblotting assay

Proteins were extracted in radioimmunoprecipitation assay buffer (150 mM NaCl, 50 mM Tris, 2 mM EGTA, 2 mM EDTA, 25 mM NaF, 25 mM glycerophosphate, 0.2% Triton X-100, 0.3% NONIDET P-40, 0.1 mM PMSF). And nuclear proteins were extracted following the protocol of the nuclear protein extraction kit following (Gerneray Technology, CN). 40.0 µg of total protein was loaded per lane. Proteins were fractionated on 10% Tris-glycine pre-cast gels (Novex, USA), transferred to a nitrocellulose membrane (Millipore Corporation, USA), and probed with primary antibodies and then HRP-labeled secondary antibodies. Proteins were visualized using ECL (Wang et al. 2009).

#### 4.8. Densitometric analysis

Results were quantified using the Quantity One version densitometry analysis software (Bio-Rad Laboratories), and expressions of proteins above were calculated. Cells treated with DMSO (0.002%) were standard as 1-fold. The results shown were pooled data of three independent experiments.

#### 4.9. Real-time quantitative PCR assay

Total RNA was extracted using the Trizol reagent (Bio Basic Inc., Markham, Ontario, Canada) and cDNA was synthesized using 2.0 µg of total RNA with random hexamer primers and RevertAid™ M-MuLV Reverse Transcriptase (Fermentas International Inc., Canada). Equilibrated amounts of cDNA were taken for transcript PCR amplification, which was performed using QuantiTect™ SYBR Green PCR kits (Qiagen Inc., USA). The house-keeping gene GAPDH was used as an internal standard. Primers used for the PCR were as follows: p21: 5'-GAGCGATGGAACCTCGACTTT-3' and 5'-TAGAGSGTTCTCTTCGCGG-3' GAPDH: 5'-GTCATCCATGACAACTTTGG-3' and 5'-GAGCTTGACAAAGTGGTCTGT-3'. The PCR protocol consisted of thermal cycling as follows: initial denaturation at 95 °C for 15 min, followed by 40 cycles of 95 °C for 30 s, 56 °C for 30 s, and 72 °C for 30 s using an Eppendorf epGradient Mastercycler (Eppendorf, Hamburg, Germany). In all experiments, two negative controls were carried through all steps. Data quantitation was performed using the relative standard curve method.

#### 4.10. Statistical analysis

Data were expressed as the mean ± SD from at least three separate experiments, and normalized to Control, and statistical significance was assessed by Student's two-tailed unpaired t-test. (\*\*p < 0.01 and \*\*\*p < 0.001.)

Acknowledgements: This study was supported by grants from the National Natural Science Foundation of China (NO. 30572211 and 307725911) and Department of Education of Zhejiang Province (NO. N20080116).

#### References

Adams J, Palombella VJ, Sausville EA, Johnson J, Destree A, Lazarus DD, Maas J, Pien CS, Prakash S, Elliott PJ (1999) Proteasome inhibitors:

a novel class of potent and effective antitumor agents. *Cancer Res* 59: 2615–2622.

Armstrong M, Schumacher K, Mody R, Yanik G, Opipari AJ, Castle V (2008) Bortezomib as a therapeutic candidate for neuroblastoma. *J Exp Ther Oncol* 7: 135–145.

Boulares AH, Yakovlev AG, Ivanova V, Stoica BA, Wang G, Iyer S, Smulson M (1999) Role of poly(ADP-ribose)polymerase (PARP) cleavage in apoptosis: Caspase 3-resistant PARP mutant increases rates of apoptosis in transfected cells. *J Biol Chem* 274: 22932–22940.

Fang L, He Q, Hu Y, Yang B (2007) MZ3 induces apoptosis in human leukemia cells. *Cancer Chemother Pharmacol* 59: 397–405.

Fulda S, Debatin KM (2003) Apoptosis pathways in neuroblastoma therapy. *Cancer Lett* 197: 131–135.

Gartel AL, Tyner AL (2002) The role of the cyclin-dependent kinase inhibitor p21 in apoptosis. *Mol Cancer Ther* 1: 639–649.

Gross A, Jockel J, Wei MC, Korsmeyer SJ (1998) Enforced dimerization of BAX results in its translocation, mitochondrial dysfunction and apoptosis. *EMBO J* 17: 3878–3885.

Hengartner O (2000) The biochemistry of apoptosis. *Nature* 40: 7770–7777.

Hotz M, Gong J, Traganos F, Darzynkiewicz Z (1994) Flow cytometric detection of apoptosis: comparison of the assays of in situ DNA degradation and chromatin changes. *Cytometry* 15: 237–244.

Kang KH, Kim WH, Choi KH (1999) p21 promotes ceramide-induced apoptosis and antagonizes the antideath effect of Bcl-2 in human hepatocarcinoma cells. *Exp Cell Res* 253: 403–412.

Kim H, Rafiuddin-Shah M, Tu H, Jeffers JR, Zambetti GP, Hsieh J, Cheng EH (2006) Hierarchical regulation of mitochondrion-dependent apoptosis by BCL-2 subfamilies. *Nat Cell Biol* 8: 1348–1358.

Maheshwari A, Misro MM, Aggarwal A, Sharma RK, Nandan D (2009) Pathways involved in testicular germ cell apoptosis induced by H<sub>2</sub>O<sub>2</sub> in vitro. *FEBS* 276: 870–881.

Maris JM, Matthay KK (1999) Molecular biology of neuroblastoma. *J Clin Oncol* 17: 2264–2279.

Sheikh MS, Garcia M, Zhan Q, Liu Y, Fornace AJ (1996) Cell cycle-independent regulation of p21WAF1/CIP1 and retinoblastoma protein during okadaic acid-induced apoptosis is coupled with induction of Bax protein in human breast carcinoma cells. *Cell Growth Differ* 7: 1599–1607.

Voorhees PM, Dees EC, O'Neil B, Orlowski RZ (2003) The proteasome as a target for cancer therapy. *Clin Cancer Res* 9: 6316–6325.

Wang D, Weng Q, Zhang L, He Q, Yang B (2009) VEGF and Bcl-2 interact via MAPKs signaling pathway in the response to hypoxia in neuroblastoma. *Cell Mol Neurobiol* 29: 391–401.

Ying M, Tu C, Ying H, Hu Y, He Q, Yang B (2008) MSFTZ, a flavanone derivative, induces human hepatoma cell apoptosis via a reactive oxygen species- and caspase-dependent mitochondrial pathway. *J Pharmacol Exp Ther* 325: 758–765.

Yu Z, Li W, Lu Q, Wang L, Zhang X, Han P, Chen P, Pei Y (2008) p21 Is required for atRA-mediated growth inhibition of MEPM cells, which involves RAR. *J Cell Biochem* 104: 2185–2192.

Zhang Q, Wang L, Zhang Y, Jiang X, Yang F, Wu W, Janin A, Chen Z, Shen Z, Chen S, Zhao W (2009) The proteasome inhibitor bortezomib interacts synergistically with the histone deacetylase inhibitor suberoylanilide hydroxamic acid to induce T-leukemia/lymphoma cells apoptosis. *Leukemia* 12: 1–8.